

Flexible Piezoelectric PMN–PT Nanowire-Based Nanocomposite and Device

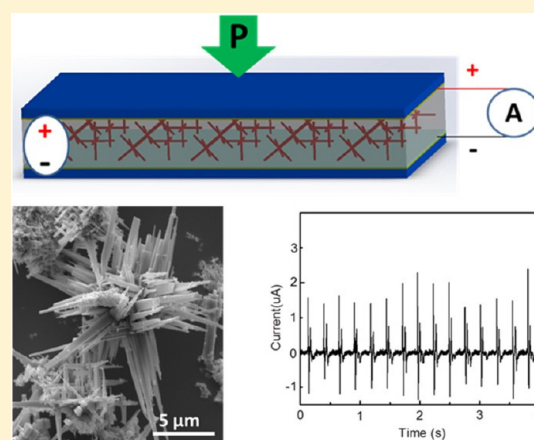
Shiyu Xu,[†] Yao-wen Yeh,^{†,‡} Gerald Poirier,[†] Michael C. McAlpine,[§] Richard A. Register,[⊥] and Nan Yao^{*,†}

[†]Princeton Institute for Science and Technology of Materials, [‡]Department of Electrical Engineering, [§]Department of Mechanical and Aerospace Engineering, and [⊥]Department of Chemical and Biological Engineering, Princeton University, Princeton, New Jersey 08544, United States

Supporting Information

ABSTRACT: Piezoelectric nanocomposites represent a unique class of materials that synergize the advantageous features of polymers and piezoelectric nanostructures and have attracted extensive attention for the applications of energy harvesting and self-powered sensing recently. Currently, most of the piezoelectric nanocomposites were synthesized using piezoelectric nanostructures with relatively low piezoelectric constants, resulting in lower output currents and lower output voltages. Here, we report a synthesis of piezoelectric $(1-x)\text{Pb}(\text{Mg}_{1/3}\text{Nb}_{2/3})\text{O}_3-x\text{PbTiO}_3$ (PMN–PT) nanowire-based nanocomposite with significantly improved performances for energy harvesting and self-powered sensing. With the high piezoelectric constant (d_{33}) and the unique hierarchical structure of the PMN–PT nanowires, the PMN–PT nanowire-based nanocomposite demonstrated an output voltage up to 7.8 V and an output current up to 2.29 μA (current density of 4.58 $\mu\text{A}/\text{cm}^2$); this output voltage is more than double that of other reported piezoelectric nanocomposites, and the output current is at least 6 times greater. The PMN–PT nanowire-based nanocomposite also showed a linear relationship of output voltage versus strain with a high sensitivity. The enhanced performance and the flexibility of the PMN–PT nanowire-based nanocomposite make it a promising building block for energy harvesting and self-powered sensing applications.

KEYWORDS: PMN–PT nanowires, piezoelectric nanocomposite, energy harvesting, nanogenerators, self-powered sensors



Piezoelectric nanostructures have attracted extensive attention because they can provide a practical way to scavenge energy from the environment to power nanodevices and nanosystems. They can also be used as novel self-powered sensing devices. A variety of piezoelectric nanostructures, such as ZnO nanowires,¹ BaTiO₃ thin films,² lead zirconium titanate (PZT) nanofibers,³ and polyvinylidene difluoride (PVDF) nanofibers⁴ have been used to convert mechanical energy into electricity. Devices based on ZnO nanowires and PZT nanofibers/nanowires have also been demonstrated as mechanical sensors^{5–8} and biosensors.⁹ However, piezoelectric ceramic materials are quite brittle; this increases the difficulty in device integration since the fabrication process is often very complex. Recently, there have been attempts to fabricate piezoelectric nanocomposites in which a flexible matrix prevents the breaking and cracking of embedded piezoelectric nanowires under mechanical stress. For example, a flexible nanocomposite based on BaTiO₃ nanoparticles mixed with graphitic carbon has been developed as a promising candidate for energy harvesting.¹⁰ Another example is a NaNbO₃ nanowire-based piezoelectric nanocomposite, which has been

demonstrated for powering small electronic devices such as light-emitting diodes (LEDs).¹¹

The piezoelectric coupling coefficient (d_{33}), which represents the ability of piezoelectric materials to convert mechanical deformation into an electric signal, plays a key role in the device performance. BaTiO₃ and NaNbO₃ based piezoelectric nanocomposites have limited output voltage and current due to their relatively low piezoelectric coefficients. Materials with high piezoelectric constants are highly desired for applications of piezoelectric materials. One such material is the new single-crystal piezoelectric $(1-x)\text{Pb}(\text{Mg}_{1/3}\text{Nb}_{2/3})\text{O}_3-x\text{PbTiO}_3$ (PMN–PT), which has a piezoelectric coupling coefficient (d_{33}) up to 2500 pm/V¹² and much higher than that of conventional ceramics. For example, the piezoelectric coupling coefficient (d_{33}) of single-crystal bulk PMN–PT is almost 30 times higher than that of BaTiO₃, which is approximately 85.3 pm/V,¹³ and almost 4 times higher than that of PZT bulk material. The piezoelectric coupling coefficient (d_{33}) of PMN–

Received: January 14, 2013

Revised: April 17, 2013

Published: May 1, 2013

PT nanowires synthesized recently by our group was measured as 371 pm/V.¹⁴ This is over 13 times higher than that of BaTiO₃ nanoparticles and 90 times higher than that of NaNbO₃ nanowires, which are approximately 28 and 4 pm/V, respectively.^{15,16} A theoretical prediction has suggested that PMN–PT nanowires could generate high output power with higher efficiency than other piezoelectric nanostructures.¹⁷ On the other hand, another profound way to increase the output voltage and/or power of piezoelectric nanocomposites is to modify the surface of the nanostructures or use special nanostructures to enhance the efficiency with which the matrix can transfer stress to its active inclusions, such as piezoelectric nanowires. Therefore, a novel piezoelectric nanocomposite containing unique PMN–PT nanostructures would have great potential for high-power nanogenerators and large-output signal sensors with lightweight, flexibility, and low cost.

In this paper, we report a novel piezoelectric nanocomposite based on hierarchical PMN–PT nanowires synthesized using a hydrothermal process. Each individual nanowire is grown with a single crystalline orientation. These nanowires were mixed with polydimethylsiloxane (PDMS) to produce a piezoelectric nanocomposite. The nanocomposite slurry was spin-casted onto a metal-coated plastic substrate and subsequently cured. Voltage and current generation of the PMN–PT nanocomposite were measured during a mechanical tapping. The performance of the piezoelectric PMN–PT nanocomposite as a self-powered sensor was demonstrated using a dynamic mechanical analyzer. This PMN–PT nanocomposite produced much higher output voltage and current than other reported piezoelectric nanocomposites, as a result of both the high piezoelectric coefficient and the unique hierarchical structure of the PMN–PT nanowires. The PMN–PT nanocomposite also exhibited a linear and sensitive dependence of output voltage on strain, indicating its potential as a flexible self-powered sensor.

Our synthesis of hierarchically structured PMN–PT nanowires is based on a versatile hydrothermal method to synthesize ceramic nanoparticles and nanowires.^{18,19} PMN–PT sol–gel was prepared by the method described in ref 14. Ten milliliters of PMN–PT sol–gel was dispersed into distilled (DI) water with strong stirring to form a 60 mL solution. Poly(acrylic acid), 0.05 g, was then added to the yellow solution. Then 15 g of KOH was slowly added into the yellow homogeneous solution and a white precipitate was formed. The final product was introduced into an autoclave (80 mL in volume), sealed, and kept in an oven at 200 °C for 24 h. After cooling to room temperature, the yellow suspension was washed with DI water and ethanol 6 times and dried at ~100 °C in an oven overnight. Light yellow powder consisting of PMN–PT nanowires was obtained.

The hierarchical PMN–PT nanowires were mixed with PDMS (Dow Corning Sylgard 184, premixed with curing agent in a ratio of 10:1 w/w, and degassed) in a ratio of 1:10 w/w by a mechanical mixing. The well-mixed slurry was spin-casted onto a Ti/Au (10/100 nm) coated polyimide film. After curing at 150 °C for 30 min, another piece of Ti/Au coated polyimide film was attached to the PMN–PT nanocomposite using a thin layer of PDMS with the metal coating facing the nanocomposite and cured at same temperature. Pt leads were then bonded to the two metal electrodes using silver paste. Finally, the device based on the hierarchical PMN–PT nanowire composite was poled with an electric field of 5 kV/mm at 150 °C in a silicone oil bath for 24 h. Periodic step strains (5 Hz)

were applied to the nanocomposite device using a TA Instruments RSA-III in the three-point bending mode.

Figure 1 shows typical scanning electron microscopy (SEM) images of the obtained PMN–PT nanowires. Figure 1a reveals

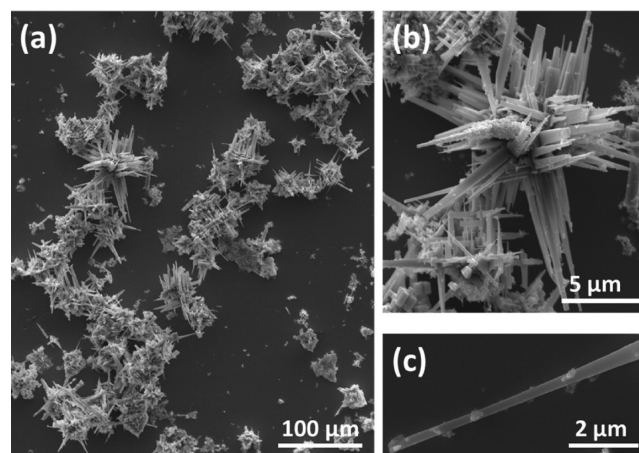


Figure 1. SEM images of hierarchical PMN–PT nanowires. (a) Low-magnification SEM image of dispersed PMN–PT nanowires. (b) High-magnification SEM image of a randomly selected nanowire bundle. (c) SEM image of a single PMN–PT nanowire.

that the product obtained from the hydrothermal synthesis consists of a large quantity of nanowires in an over 80% yield; the byproduct is in nanoparticle form. Figure 1b is a higher-magnification SEM image of a randomly selected nanowire bundle. These bundles show a fern-branch three-dimensional (3D) hierarchical structure with individual nanowires extending in various directions. The length of individual nanowires is up to 10 μm. The size of an individual nanowire varies along its longitudinal growth direction, as shown in Figure 1c, which ranges from about 200 to 800 nm. Some nanowires also have needlelike ends. The cross-section of individual nanowires is rectangular, which differs from other piezoelectric nanostructures such as ZnO and PZT. X-ray diffraction (XRD), as shown in Supporting Information Figure S1, indicates that these nanostructures have a perovskite (monoclinic) structure with lattice constants $a = 4.03 \text{ \AA}$, $b = 4.00 \text{ \AA}$, and $c = 4.02 \text{ \AA}$, consistent with the structure of PMN–PT thin films.²⁰

A dark-field transmission electron microscopy (TEM) image taken from a randomly selected nanowire is presented in Figure 2a. This low-magnification image shows that the nanowire has a tapering width along its length, decreasing from 697 to 394 nm along the growth direction (as marked by the white arrow, which is shown below to be the [100] direction). Furthermore, the entire nanowire shows a continuous bright contrast, indicating that there are no obvious defects in the nanowire. The bright-field TEM image of another PMN–PT nanowire is shown in Figure 2b, again revealing a tapering along the growth direction, from 201 to 157 nm. The selected area electron diffraction (SAED) pattern along the [110] direction shown in Figure 2c indicates that the PMN–PT nanowire is structurally uniform and with a single crystalline orientation. This is further demonstrated by a high-resolution TEM image shown in Figure 2d, demonstrating that the PMN–PT nanowire is single-crystalline with a near-perfect crystal structure. A higher-magnification lattice image is shown in Figure 2e. The 4.03 Å lattice spacing corresponds to the (100) lattice plane, indicating this nanowire grew along the [100] direction, while the lattice

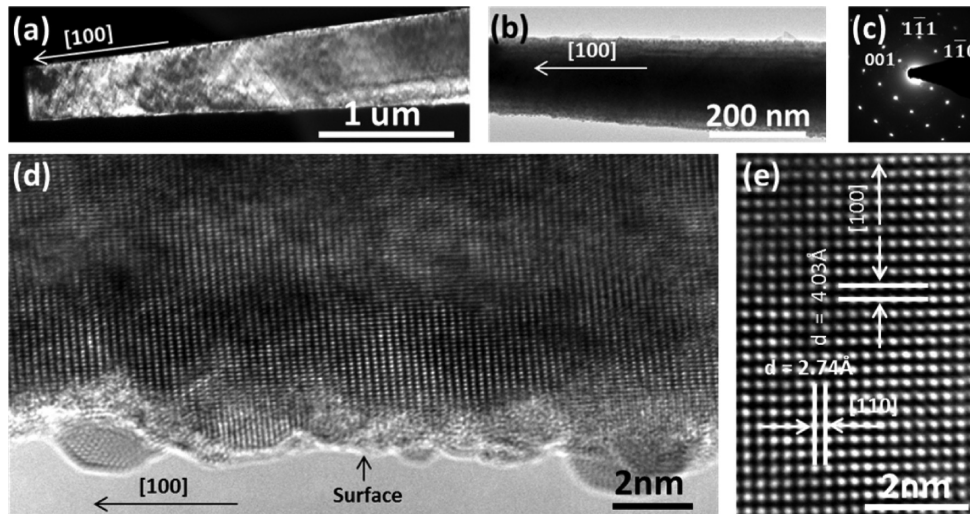


Figure 2. TEM images of a single PMN–PT nanowire. (a) Dark-field TEM image. (b) Bright-field TEM image. (c) SAED pattern along the [110] direction. (d) HRTEM image. (e) Higher-magnification HRTEM image.

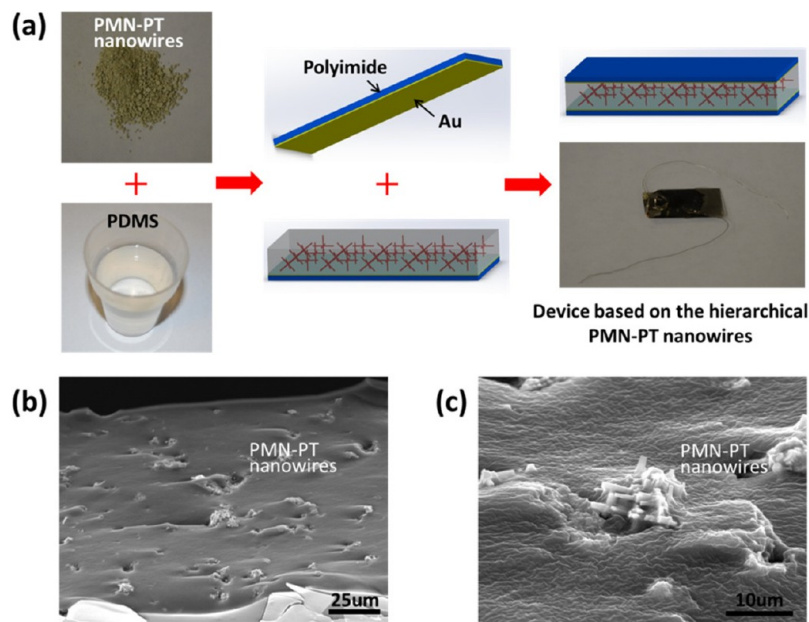


Figure 3. Fabrication process for the PMN–PT nanowire-based nanocomposite and device. (a) Photos of the PMN–PT nanowires, PDMS, and final device, as well as schematics of the electrodes and device. (b) SEM image of the cross-section of the PMN–PT nanocomposite. (c) SEM image of an individual hierarchical PMN–PT nanowire structure embedded in PDMS.

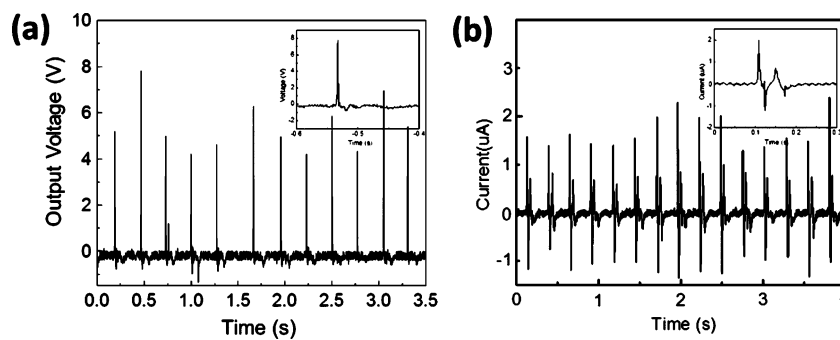


Figure 4. Signal generation from PMN–PT nanowire-based nanocomposite. (a) Voltage generation under a periodic mechanical tapping. (b) Corresponding current generation.

spacing of 2.74 Å belongs to the (110) lattice plane which is normal to the growth direction.

Figure 3a describes the fabrication process of the PMN–PT piezoelectric nanocomposite, as well as the device that is used to demonstrate signal generation and sensing. The PMN–PT nanowires are thoroughly mixed with PDMS with a ratio of 1:10. The resulting slurry is then spin-casted onto a polyimide film with a Ti/Au coating, followed by curing at 150 °C. Another piece of coated polyimide film is then placed on top of the nanocomposite with a very thin layer of PDMS and cured. The nanocomposite is thus sandwiched between two Au electrodes, which are then bonded with two electrical leads using silver paste. The final geometry of the nanocomposite part of the device is 1 cm (*L*) × 0.5 cm (*W*) × 150 μm (*T*). The device is polarized by applying 5 kV/mm DC across the electrodes in a silicone oil bath at 150 °C for 24 h. Figure 3b is a cross-sectional view of the nanocomposite, indicating that the PMN–PT nanowires are well-distributed throughout the PDMS matrix. The higher-magnification SEM image shown in Figure 3c reveals an individual hierarchical PMN–PT nanowire structure embedded in the PDMS matrix, indicating that the nanowires maintain their hierarchical form after mixing with PDMS and curing. The hierarchical PMN–PT nanowires generate electric potential under an external stress and serve as an energy generation source.

Voltage and current generation of the PMN–PT nanocomposite are assessed by tapping the device vertically using the plastic handle of a screwdriver, a simple method representative of the actual application of energy-harvesting piezoelectric generators. Figure 4a presents a typical voltage generation graph of the PMN–PT nanocomposite device. Under mechanical tapings, the device repeatedly generates voltages ranging from 4.2 to 7.8 V in an open circuit. The insert in Figure 4a is a magnified voltage output signal. The large positive peak is generated from the direct impact of the stress. The following negative peak corresponds to the damping effect occurring when the device changes from a compressed state to a relaxed state after removing the initial stress. Since the PMN–PT composite is polarized in one direction, the positive peak is always greater than the negative peak. Figure 4b shows a typical current generation graph, where the PMN–PT nanocomposite device consistently generates a positive current ranging from 1.58 to 2.29 μA and a negative current between 0.7 and 1.36 μA. The insert in Figure 4b is a magnified current output signal. Comparing Figure 4 panel b to panel a, it is seen that the difference between the positive and the negative voltage peaks is much greater than the difference between the current peaks. This is because the piezoelectric PMN–PT nanocomposite device is also a capacitor. When a piezoelectric voltage is generated, induced charges are stored on the surface of the electrodes. These stored charges then will be consumed if an opposite voltage is applied. Therefore, the measured negative voltage is always much smaller than the positive voltage. The induced current only depends on the strength of the piezoelectric potential, the piezoelectric potentials generated by the direct impact and the relaxed stress from the damping effect have no significant difference, therefore the difference of the positive current and negative current is not so obvious. To confirm that the output signals were truly generated by the PMN–PT nanocomposite, a switching-polarity test was performed. As shown in Supporting Information Figure S2a, when a current meter is connected to a PMN–PT nanocomposite device in the forward direction, a positive signal

appeared first, followed by a smaller negative signal induced by the damping effect. In the case of the reverse connection, as shown in Supporting Information Figure S2b, a negative current was generated first and a smaller positive signal appeared afterward.

Both output voltage and current from this device are greater than that generated by other reported piezoelectric nanocomposites. For example, the maximum voltage of 7.8 V is over 2 times larger than that of nanocomposite devices based on BaTiO₃ nanoparticles and NaNbO₃ nanowires, which is 3.2 V. The maximum current of 2.29 μA is over 6 times larger than that of a BaTiO₃ nanoparticle-based nanocomposite and over 30 times larger than that of a NaNbO₃ nanowire-based nanocomposite, which are 350 and 72 nA, respectively.^{10,11} The current density of this PMN–PT nanocomposite based device is about 4.58 uA/cm², which is 2 orders of magnitude higher than that of BaTiO₃ and NaNbO₃ nanostructure based nanocomposites ranging from 5 to 16 nA/cm². The current density of the PMN–PT nanowire composite based device is also 15% higher than that of well-aligned single crystal PZT nanowire array based device,²¹ which is 4 μA/cm².

The significant enhancements of the output voltage and current density could be explained by the voltage/power generation mechanism of piezoelectric nanocomposites illustrated in Supporting Information Figure S3a. An external mechanical stress is transferred through the PDMS matrix, inducing a stress in the piezoelectric nanostructures, and thereby generating an electric potential gradient along the direction of the mechanical stress. This piezoelectric potential will be transferred to the parallel electrodes and can be applied to an external circuit. The voltage generated by the piezoelectric composite, V_{out} , can be calculated as

$$V_{\text{out}} = \int g_{33} \varepsilon(l) E_p dl \quad (1)$$

where g_{33} is the piezoelectric voltage constant, which is proportional to the piezoelectric coupling coefficient (d_{33}), $\varepsilon(l)$ is the strain, and E_p is the Young's modulus. The direction l referred here is perpendicular to the electrodes. According to eq 1, V_{out} depends on three different parameters, g_{33} , $\varepsilon(l)$ and integration of dl . The first merit of PMN–PT nanowires for piezoelectric applications is their high piezoelectric constant (d_{33}), which corresponds to a high g_{33} following $g_{33} = d_{33}/\varepsilon_0 \bullet K$, where ε_0 is the permittivity of free space and K is the relative dielectric constant of the material. Further, the unique hierarchical structure could greatly contribute to their function as the active material in a piezoelectric nanocomposite. When the hierarchical PMN–PT nanowires are embedded in a PDMS matrix, the best performance will be from the alignment shown in Supporting Information Figure S3b, where some nanowires are perpendicular to the two electrodes. For this alignment, the integration of dl presented in eq 1 would be the total length of the two nanowires, thereby generating the largest output signal. A single nanowire may also have the same integration of dl , but since the Young's modulus of inorganic nanowires is many orders of magnitude larger than that of the PDMS matrix, a direct mechanical impact cannot be effectively transferred to an isolated nanowire. In the case of hierarchical PMN–PT nanowires, when some nanowires are perpendicular to the two electrodes the nanowires normal to them will serve as anchor sites that can significantly enhance the efficiency of the mechanical impact transfer, which corresponds to a high $\varepsilon(l)$. The detrimental alignment will be when no nanowire is

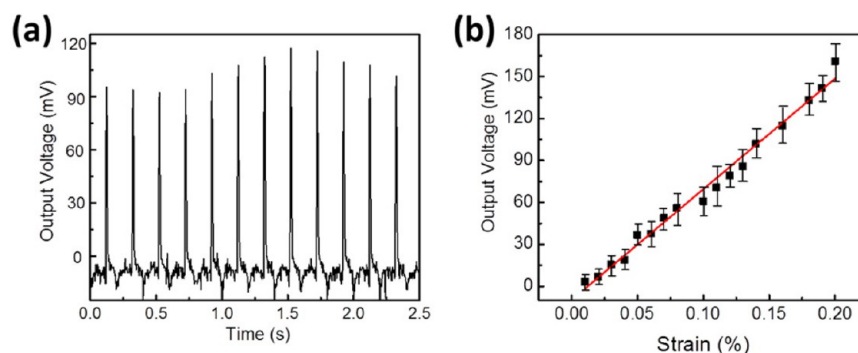


Figure 5. Sensing performance of the PMN–PT nanowire-based nanocomposite device. (a) Typical output voltage signal under periodic applied step strains. (b) Corresponding output voltage versus strain characteristics.

perpendicular to the electrodes, but the smallest angle is 54.7° , which is roughly the angle between the six crystal growth directions belonging to $\langle 100 \rangle$ orientation and crystal planes $\{111\}$, as shown in Supporting Information Figure S3c, so the total integration of dl would be the total length of two nanowires multiplied by $\sin 54.7^\circ$. If individual nanowires were used, when the nanowire is parallel to the electrodes, the integration of dl would be the diameter of the nanowire which is in the range of hundreds of nanometers, much smaller than the effective length of the hierarchical structures. This means the hierarchical PMN–PT nanowires could have a higher effective length (the integration of dl along the polarization direction or the stress direction). Therefore, the significant performance improvement in the nanocomposite device based on hierarchical PMN–PT nanowires may be attributed to both the higher piezoelectric constant and the unique hierarchical structure. One thing worth mentioning is that when piezoelectric material embedded in a polymer matrix, the effective dielectric constant (K) is lower than that of the corresponding pure piezoelectric material.²² Therefore, the higher output voltage of the PMN–PT nanocomposites based device may also attribute to the lower dielectric constant.

The mechanical sensing performance of the PMN–PT nanocomposite device was demonstrated by applying periodic strains using a dynamic mechanical analyzer (DMA). The output voltage signal under such periodic strain is shown in Figure 5a. The output voltage has the same frequency as that of the applied strain, which is 5 Hz. The output voltage ranges from 92–118 mV. The relationship between output voltage and strain is shown in Figure 5b, showing that the output voltage increases linearly with strain. The lowest strain that the PMN–PT nanocomposite device can detect is approximately 0.01%, showing that this device has promise as a highly sensitive and self-powered dynamical mechanical sensor.

In summary, a novel piezoelectric nanocomposite based on hierarchical PMN–PT nanowires has been fabricated. A maximum output voltage of 7.8 V and output current of 2.29 μA were obtained from a device based on the PMN–PT nanocomposite; this output voltage is more than double that of other reported piezoelectric nanocomposites, and the output current is at least 6 times greater. The PMN–PT nanocomposite device also shows a linear relationship of output voltage versus strain with a high sensitivity. The superior performance of the PMN–PT nanocomposite may be attributed to both the high piezoelectric constant and the unique hierarchical structures of the PMN–PT nanowires. The enhanced performance and the flexibility of the PMN–PT

nanocomposite make it a promising building block for energy harvesting and self-powered sensing applications.

■ ASSOCIATED CONTENT

Supporting Information

Additional figures. This material is available free of charge via the Internet at <http://pubs.acs.org>.

■ AUTHOR INFORMATION

Corresponding Author

*E-mail: nyao@princeton.edu.

Notes

The authors declare no competing financial interest.

■ ACKNOWLEDGMENTS

This work is supported in part by the National Science Foundation-MRSEC program through the Princeton Center for Complex Materials (DMR-0819860).

■ REFERENCES

- (1) Wang, Z. L.; Song, J. H. *Science* **2006**, *312*, 242–246.
- (2) Park, K. I.; Xu, S.; Liu, Y.; Hwang, G. T.; Kang, S. J.; Wang, Z. L.; Lee, K. J. *Nano Lett.* **2010**, *10*, 4939–4943.
- (3) Chen, X.; Xu, S. Y.; Yao, N.; Shi, Y. *Nano Lett.* **2010**, *10*, 2133–2137.
- (4) Chang, C.; Tran, H. V.; Wang, J. B.; Fuh, Y. K.; Lin, L. W. *Nano Lett.* **2010**, *10*, 726–731.
- (5) Xiao, X.; Yuan, L. Y.; Zhong, J. W.; Ding, T. P.; Liu, Y.; Cai, Z. X.; Rong, Y. G.; Han, H. W.; Zhou, J.; Wang, Z. L. *Adv. Mater.* **2011**, *23*, 5440–5444.
- (6) Chen, X.; Li, J. W.; Zhang, G. T.; Shi, Y. *Adv. Mater.* **2011**, *23*, 3965–3969.
- (7) Cohen-Tanugi, D.; Akey, A.; Yao, N. *Nano Lett.* **2010**, *10*, 852–859.
- (8) Xu, S. Y.; Poirier, G.; Yao, N. *Nano Energy* **2012**, *1*, 602–607.
- (9) Nguyen, T. D.; Deshmukh, N.; Nagaraj, J. M.; Kramer, T.; Purohit, P. K.; Berry, M. J.; McAlpine, M. C. *Nat. Nanotechnol.* **2012**, *7*, 587–589.
- (10) Park, K. I.; Lee, M.; Liu, Y.; Moon, S.; Hwang, G. T.; Zhu, G.; Kim, J. E.; Kim, S. O.; Kim, D. K.; Wang, Z. L.; Lee, K. J. *Adv. Mater.* **2012**, *24*, 2999–3004.
- (11) Jung, J. H.; Lee, M.; Hong, J. I.; Ding, Y.; Chen, C. Y.; Chou, L. J.; Wang, Z. L. *ACS Nano* **2011**, *5*, 10041–10046.
- (12) Fu, H. X.; Cohen, E. R. *Nature* **2003**, *403*, 281–283.
- (13) Berlincourt, D.; Japze, H. *Phys. Rev.* **1958**, *111*, 143–148.
- (14) Xu, S. Y.; Poirier, G.; Yao, N. *Nano Lett.* **2012**, *12*, 2238–2242.
- (15) Deng, Z.; Dai, Y.; Chen, W.; Pei, X.; M.; Liao, J. H. *Nanoscale Res. Lett.* **2010**, *5*, 1217–1221.
- (16) Ke, T. Y.; Chen, H. A.; Sheu, H. S.; Yeh, J. W.; Lin, H. N.; Lee, C. Y.; Chiu, H. T. *J. Phys. Chem. C* **2008**, *112*, 8827–8831.

- (17) Sun, C. L.; Shi, J.; Wang, X. D. *J. Appl. Phys.* **2010**, *108*, 034309–034320.
- (18) Lu, C. H.; Qi, L. M.; Yang, J. H.; Tang, L.; Zhang, D. Y.; Ma, J. *M. Chem. Commun.* **2006**, 3551–3553.
- (19) Babooram, K.; Ye, Z. G. *Chem. Mater.* **2004**, *16*, 5365–5372.
- (20) Wang, J.; Stampfer, C.; Roman, C.; Ma, W. H.; Setter, N. *Appl. Phys. Lett.* **2008**, *93*, 223101–22310.
- (21) Xu, S.; Henson, J. B.; Wang, Z. L. *Nature Commun.* **2010**, DOI: 10.1038/ncomms1098.
- (22) Chan, H. W.; Unsworth, J. *IEEE Trans. Ultrason. Ferroelectr. Freq. Control* **1989**, *36*, 434–441.